CARBON 67 (2014) 680–687

Available at www.sciencedirect.com

ScienceDirect

journal homepage: www.elsevier.com/locate/carbon

Single-step CVD growth of high-density carbon nanotube forests on metallic Ti coatings through catalyst engineering

Guofang Zhong *, *Rongsi Xie*, *Junwei Yang*, *John Robertson*

Department of Engineering, University of Cambridge, Cambridge CB3 0FA, UK

ARTICLE INFO

Article history:
Received 17 May 2013
Accepted 21 October 2013
Available online 29 October 2013

ABSTRACT

We demonstrate the direct growth of carbon nanotube (CNT) forests on metallic titanium (Ti) coatings by single-step chemical vapor deposition. This was achieved by catalyst engineering, which involves a novel design of Fe/Ti/Fe nanostructure sputtering coated on SiO_2/Si wafers. The Fe sublayer, an additional catalyst added to the conventional catalyst/support design, plays a key role in the growth of well aligned and highly dense CNT forests. Depth profile analysis of substrates by secondary ion mass spectroscopy shows that the Fe sublayer is thermally unstable at the Ti/SiO_2 interface under the growth conditions. Catalyst diffusion back to the surface from the Fe sublayer is much more significant than down towards the SiO_2/Si substrate from the surface Fe layer. This makes it possible to minimize the thickness of surface catalyst layer, and ensures the growth of well aligned and high-density CNT forests on Ti coatings. The filling factor of nanotubes on the substrate after liquid-induced compaction can be dramatically increased up to 57%, leading to an estimation of the areal density of around 10^{12} cm^{-2}.

1. Introduction

Currently, the most efficient way to produce vertically aligned carbon nanotubes (CNTs) is catalytic chemical vapor deposition (CVD) [1–7]. First, it usually involves the deposition of a thin catalyst layer as well as an underneath oxide support. A transition metal such as Fe, Co, Ni or their alloys is commonly used as catalyst, while Al_2O_3, MgO and SiO_2 are the best oxide supports [8–11]. Then, a CVD pre-treatment or annealing is employed to convert the catalyst layer into active nanoparticles through catalyst reduction and dewetting. Finally, CVD growth of vertically aligned CNTs is carried out with a hydrocarbon source gas such as ethylene or acetylene, usually diluted in hydrogen or inert gases. The catalyst–oxide support interactions restrict the catalyst surface mobility, stabilizing small catalytic nanoparticles at elevated CVD temperatures and leading to a high nucleation density of CNTs. In recent years, great progress has been achieved in the growth of high-density (10^{12}–10^{13} cm^{-2}) single-walled CNT (SWCNT) forests on Al_2O_3 support [12–15]. However, it is still challenging to reproduce the high-density CNT forests on conductive supports, especially on transition metal supports such as Cu, Ti and Ta. This is needed because of an urgent demand for nanotube applications as interconnects [16–18].

Studies have shown that the thickness of the surface catalyst has a decisive effect on the diameter and density of the as-grown CNT forests; the thickness of the surface catalyst should be prepared as thin as possible in order to increase the CNT density [11,14]. In the case of a metal support, the challenges lie in: (1). A metal support has higher surface energy than an oxide support [19,20], so that it is more difficult

* *Corresponding author.*
E-mail addresses: gz222@cam.ac.uk, zhongchina@msn.com (G. Zhong).
0008-6223/$ - see front matter
http://dx.doi.org/10.1016/j.carbon.2013.10.057

to form high-density and small catalytic nanoparticles on the metal surface through dewetting under the growth temperature. (2). The catalyst-support-gas interactions are more complicated [21,22]. The support may easily form alloys with the catalyst, and its grain may get coarsened during the CVD process [21]. In addition to Ostwald ripening and subsurface diffusion [8–10], alloying and grain boundary diffusion make the catalyst loss on the surface even faster. Furthermore, the metal support may also interact with the feeding and/or residual gases to form carbides and/or oxides, which significantly inhibit the growth of CNT forests and affect the contact between nanotubes and the support.

During the past decade, attempts have been made toward the growth of CNT forests on various metal substrates by different CVD methods [18,19,23–30]. However, the density and alignment of CNTs are far below that of the date-of-the-art high-density SWCNT forests grown on the Al_2O_3 support. Furthermore, most of the processes commonly use the Al_2O_3 coating (or Al coating, on which a passive oxide layer should be formed on exposure to air) between the catalyst and the metal support as a barrier layer [23–29]. In order to reduce the contact resistance between the nanotube and the support, it is essential to grow CNT forests directly on metal supports without the assistance of any insulating oxide coatings. Recently, encouraging progress has been made [18,31–33]. Esconjauregui et al. succeeded in growing multi-walled CNT (MWCNT) forests (4×10^{11} cm^{-2}) on conductive substrates by tuning the nominal thickness of the Al_2O_3 support down to 0.5 nm, which allows a good electrical contact through tunneling [33]. Yamazaki et al. reported the growth of almost closely packed MWCNT forests (1×10^{12} cm^{-2}) on 10 nm TaN by a multi-step growth method using plasma-assisted CVD [31]. In their process, plasma-assisted formation and immobilization of catalytic nanoparticles by a carbon film can be carried out only under very restricted pre-treatment conditions in order to obtain the high-density CNT forests during the final growth step, which are not sensitive any more to the growth temperature in a large range. Dijon et al. claimed the growth of nanotubes on metallic Al-Cu (99.5% Al) alloy with a density up to 2.5×10^{12} cm^{-2} [32]. The latter also use plasma-assisted CVD under a low pressure of 1 mbar. Very recently, Rao et al. even made a promising approach to grow CNT forests on Cu and other metals by using graphene as an atomically thin interface [34].

In this paper, we demonstrate a novel concept of catalyst engineering, which enables the growth of well aligned and high-density CNT forests on Ti coatings by using a single-step cold-wall CVD process. It requires neither a special plasma pre-treatment of catalyst nor an oxide barrier layer over the conductive support. Instead, only an additional Fe catalyst sublayer is added to the conventional catalyst/support design, i.e., we prepare δ nm Fe, 10 nm Ti and τ nm Fe sequentially by magnetron sputtering on Si wafers with 200 nm thermally grown SiO_2 as illustrated in Fig. 1a. Our purpose is to minimize and sustain the surface catalyst during CVD process through a back diffusion of catalyst from the sublayer. Experiments indicate that a proper $\tau - \delta$ combination of the two catalyst layers can dramatically enhance the growth of well aligned and high-density CNT forests.

2. Experimental

Fe and Ti were used as the catalyst and the metal support, respectively, while Si wafers with 200 nm thermally grown SiO_2 were used as the substrates. Both Fe and Ti were sputtering coated using Ar as the sputtering gas. In order to accurately control the catalyst thickness, a low sputtering rate of about 1.1 nm/min was applied by using a low sputtering power of 20 W to a 4-inch Fe target under 3.5×10^{-3} mbar. First, δ nm (0–2 nm) Fe was coated on a SiO_2/Si wafer; here, $\delta = 0$ nm means this step was skipped (equivalent to the conventional catalyst design). Following this step, 10 nm Ti and τ nm (0.5–2 nm) Fe were sequentially coated without breaking the vacuum (Fig. 1a). A single-step process was employed to grow nanotubes on the Ti coatings using a cold-wall CVD apparatus, which has been successfully used for the growth of high-density SWCNT forests [6,14]. In the CVD process, the substrates were directly heated from room temperature to growth temperature under 15 mbar, 40 sccm C_2H_2 and 460 sccm H_2, without any pre-annealing of the catalyst. The effect of pre-annealing of the substrates on the growth of nanotubes was also investigated. A method of liquid-induced compaction [35–37], which includes soaking the nanotube samples thoroughly in ethanol, and letting them dry in the air, was used to estimate the areal density of CNT forests [14,38].

The nanotube samples were characterized by scanning electron microscopy (SEM, Philips XL30 SFEG and Carl Zeiss Sigma) and high resolution transmission electron microscopy (HRTEM, FEI Tecnai F20). Element depth profile analysis on selected substrates by secondary ion mass spectroscopy (SIMS) was carried out as a service by Loughborough Surface Analysis Ltd. An ^{18}O ion beam was used for the SIMS analysis. The electrical measurements were carried out on selected samples with a two-point probe station (Keithley 4200-SCS). In order to get a good contact, 50 nm Au was pre-coated on selected substrates after the catalyst preparation and before the CVD growth of nanotubes. The probe spacing was set to a constant of 5 mm.

3. Results and discussions

3.1. *Effect of catalyst engineering on CNT growth*

Fig. 1 demonstrates that our novel catalyst design of τ nm Fe/10 nm Ti/δ nm Fe/SiO_2/Si can significantly enhance the growth of CNT forests on the Ti coating. Fig. 1(b–d) are nanotubes grown on substrates with the conventional catalyst design ($\delta = 0$); Fig. 1(e–l) are nanotubes obtained from our novel catalyst design but with different $\tau - \delta$ combinations. All the samples were produced by the single-step CVD at 15 mbar, 40 sccm C_2H_2, 460 sccm H_2 and 700 °C, however, (b–h) were prepared in 10 min while (i–l) in 6 min. It can be seen that only disordered or less aligned nanotubes could be grown on the Ti coating without a catalyst sublayer; in contrast, aligned CNT forests could be prepared using our novel catalyst design. This proves that the catalyst sublayer plays a very important role in the growth of aligned CNT forests on the Ti coating. It can be also seen from Fig. 1(j and k) that the thin Fe sublayer in the range of 0.6–0.8 nm gives the best alignment of CNT forests. As CNT alignment is caused by a crowding effect of

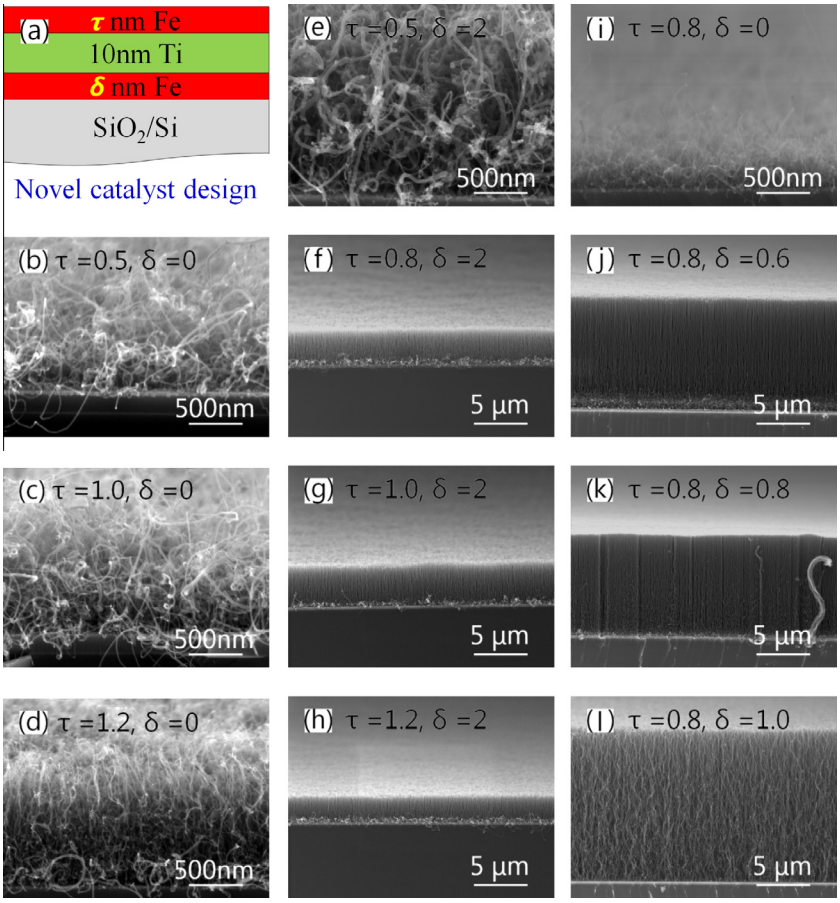

Fig. 1 – Comparative growth of carbon nanotubes on Ti coatings using the conventional and our novel catalyst designs, respectively. (a) Schematic diagram of our novel catalyst design of τ nm Fe/10 nm Ti/δ nm Fe on SiO_2/Si; it is equivalent to the conventional catalyst design if $\delta = 0$. (b–l) Cross-sectional SEM images of nanotubes grown on Ti coatings with different $\tau - \delta$ combinations. All the samples were produced by the single-step CVD at 15 mbar, 40 sccm C_2H_2, 460 sccm H_2 and 700 °C, however, (b–h) were prepared in 10 min while (i–l) in 6 min. (A colour version of this figure can be viewed online.)

nanotubes [39], better alignment usually also means higher nanotube density if the nanotube diameter keeps the same [40]. An Fe sublayer thicker than 1.0 nm will produce nanotubes with larger diameters observed by SEM at high magnifications.

The electrical properties of the bare substrates and the as-grown high-density CNT samples were measured by using a two-point probe station. Fig. 2 shows the characteristic I–V curves and the derived resistances. The insets in Fig. 2 illustrate how to contact the probes with samples. The overall resistance derived from an I–V curve includes not only the resistances of the as-grown nanotubes and the substrates, but also the contacts of probe to nanotube, nanotube to Ti, and/or probe to Au, Au to Ti. The I–V curve of the as-deposited bare substrate (coated with 0.8 nm Fe/10 nm Ti/0.8 nm Fe on SiO_2) gives an electrical resistance about 180–195 Ω, similar to that of a conductive $CoSi_2$ coating [19]. However, an annealing of the substrate in 15 mbar pure H_2 at 700 °C for 6 min resulted in an increase of the resistance to more than 10 kΩ, as can be seen in Fig. 2(a and b). This implies that the Ti coating can also be partially oxidized under high temperature by the residual O_2/H_2O in the CVD system even in a reducing environment just like a Ta coating [22]. To our surprise, the as-grown CNT forests showed almost linear I–V curves by contacting the two probes with CNT forests, or by contacting one probe with the forests and the other with a gold electrode (Fig. 2(c and d)). In the latter case, nanotubes surrounding the gold electrode were removed. The derived resistances are ~1 kΩ for the CNT–Au contacts and ~1.5 kΩ for the CNT–CNT contacts. Although the overall electrical resistance is similar to or up to 10 times higher than those CNTs grown on other conductive substrates [19,33,41,42], it is still very promising if considering the high resistance of the annealed substrates. This implies nanotubes would have a fairly good contact with the Ti coating and Ti carbides may be formed during the growth of nanotubes, preventing the Ti coating from oxidation to some extent.

3.2. *Depth profile analysis of selected substrates by SIMS*

In order to disclose the role of the catalyst sublayer played in the growth, SIMS depth profiles were carried out on four substrates with the conventional catalyst design of 0.8 nm Fe/10 nm Ti (/SiO_2/Si) and the novel design of 0.8 nm Fe/10 nm Ti/1.0 nm Fe (/SiO_2/Si), see Fig. 3. Two were as-deposited and two annealed. The annealing was carried out by heating the

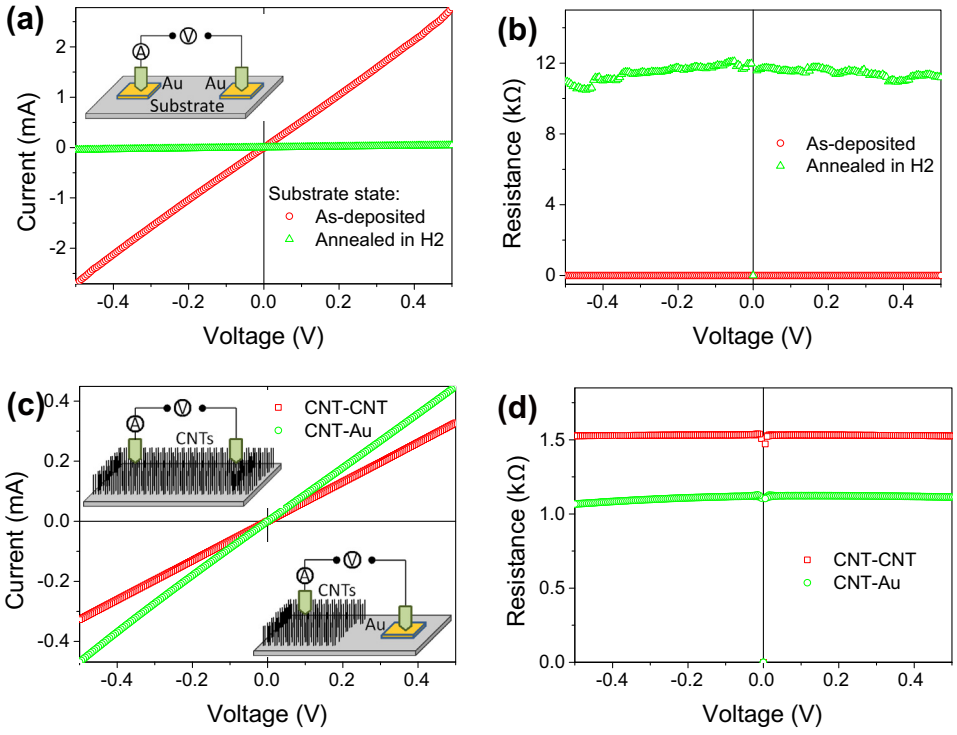

Fig. 2 – Electrical properties measured by a two-point probe station from (a–b) bare substrates coated with 0.8 nm Fe/10 nm Ti/0.8 nm Fe on SiO_2 and (c–d) the as-grown CNT forests. The insets illustrate how to contact the probes with the samples. (A colour version of this figure can be viewed online.)

substrates under 500 sccm pure H_2, 15 mbar from room temperature to 650 °C in 3 min, then switching off the heater power and letting the samples to cool down with the H_2 flow on.

As shown in Fig. 3a, for the conventional catalyst design, the abrupt and monotonous drop of the Fe signal of the as-deposited substrate (blue solid line), confirms that Fe is surface rich only. For our novel catalyst design, it is not only surface rich but also rich at the coating/SiO_2 interface as indicated by the sharp Fe peak at the interface (blue solid line) in Fig. 3b. This is just what we expected through catalyst engineering. For the conventional catalyst design, after 3 min rapid annealing, it can be seen that diffusion of Fe into the Ti coating resulted in about 40% loss of the Fe intensity on the surface. On the contrary, for our novel catalyst design, the Fe intensity on the surface increased by about 35% and the Fe peak at the coating/SiO_2 interface almost disappeared after the annealing. This strongly implies that the Fe sublayer between the Ti coating and the substrate is thermally unfavored, so that Fe diffusion back to the surface is more significant than that towards the substrate during the annealing.

It can be expected that a proper catalyst sublayer should be able to minimize and sustain the catalyst on the top surface during the nanotube growth without causing obvious loss or gain by diffusion. As the 1.0 nm Fe sublayer can already lead to the increase of surface Fe after the rapid annealing (Fig. 3b), an Fe sublayer thicker than 1.0 nm is in fact detrimental to the growth of high-density CNT forests. This is consistent with our SEM observations in Fig. 1. Experiments reveal that a catalyst combination of a 0.6–0.8 nm Fe top layer and a 0.6–0.8 nm Fe sublayer gives the best alignment of CNT forests by our single-step CVD process.

It can be noticed that the nanotubes demonstrated in Fig. 1 have different thicknesses, i.e., different growth rates. The reason is most probably related to the alignment of nanotubes. The higher is the alignment degree, the less is the strain occurred to nanotubes and the higher is the growth rate. Without the catalyst sublayer, the catalyst loses continuously through alloying and diffusion during the CVD process. This will result in a very low catalytic nanoparticle density, which may lead to the growth of low-density and randomly ordered nanotubes. If a proper catalyst sublayer exists, its back diffusion to the surface will dramatically hinder the loss of surface catalyst, which can sustain the high-density catalytic nanoparticles and lead to the growth of highly oriented high-density nanotube forests. Once the catalyst sublayer becomes too thick, its back diffusion will get too significant, which will finally result in the growth of nanotubes with large diameter, less density and less alignment.

3.3. *Effect of pre-annealing on nanoparticle formation and CNT growth*

The back diffusion of the Fe catalyst to the top surface was also confirmed by SEM observations of catalytic nanoparticles formed by a rapid annealing. Fig. 4(a–d) show the effect of 0, 0.6, 1.0 and 1.8 nm catalyst sublayers on the formation of catalytic nanoparticles; the surface catalyst and Ti layers were fixed to 0.8 and 10 nm, respectively, and the substrates were heated up from room temperature to 700 °C in 15 mbar

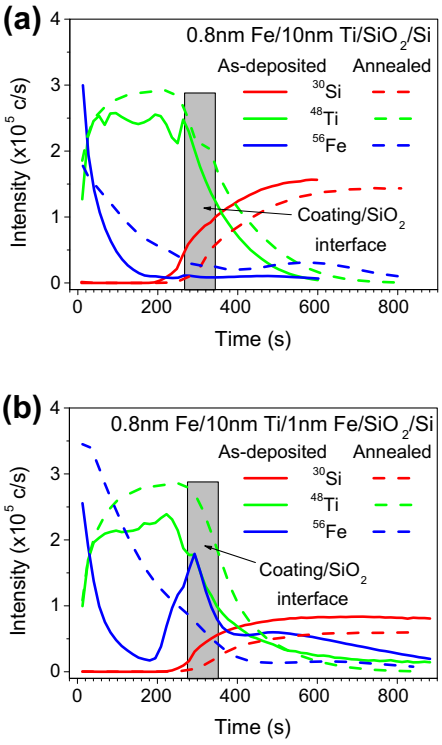

Fig. 3 – SIMS depth profiles of the as-deposited (solid lines) and annealed (dash lines) substrates with (a) the conventional catalyst design and (b) our novel catalyst design, respectively. The annealing was carried out by heating the substrates under 500 sccm pure H_2, 15 mbar from room temperature to 650 °C for 3 min, then switching off the heater power and letting the samples to cool down with the H_2 flow on. (A color version of this figure can be viewed online.)

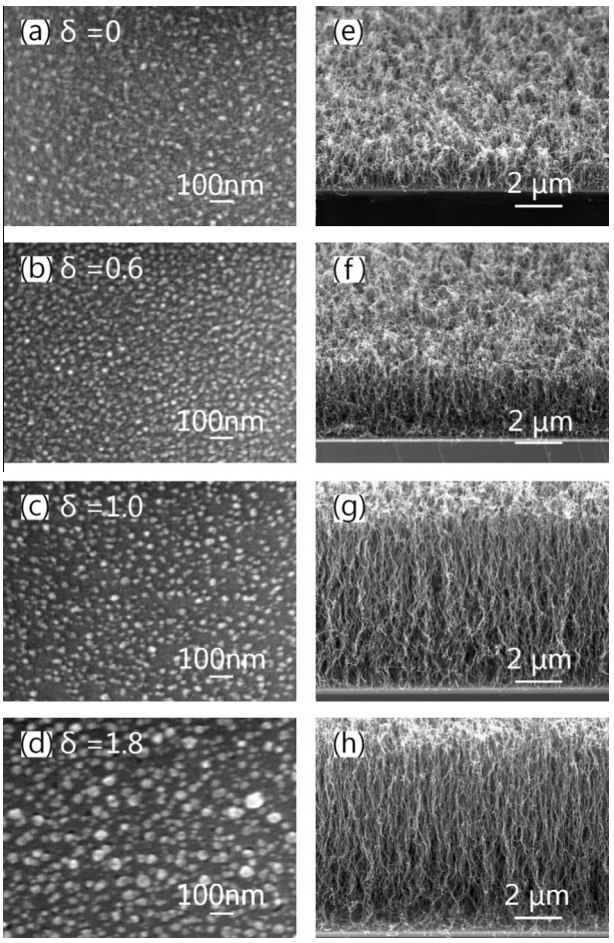

Fig. 4 – SEM observations of (a–d) catalytic nanoparticles formed by a rapid annealing and (e–h) nanotubes subsequently grown from the corresponding nanoparticles. The annealing was performed by heating the substrates under 500 sccm pure H_2, 15 mbar from room temperature to 700 °C for 3 min; the growth lasted 3 min by introducing 8% C_2H_2 in H_2 immediately after the annealing. Substrate: 0.8 nm Fe/10 nm Ti /δ nm Fe/SiO_2.

500 sccm pure H_2 for a total time of 3 min. It can be seen that a 0.6 nm Fe sublayer resulted in the highest density of catalytic nanoparticles (Fig. 4b). For the sample without a catalyst sublayer, although the catalytic nanoparticles are similar to that of the 0.6 nm Fe sublayer, but its density is much lower. This is because the surface catalyst loss is too fast without the compensation of a sublayer catalyst through its back diffusion. With the increase of sublayer thickness, catalytic nanoparticles become larger and larger, and their density becomes lower and lower. The coarsening of catalytic nanoparticles is evidence that there was a net catalyst back diffusion, which agrees well with the SIMS results.

In literature, most of the nanotubes were grown through a routine two-step CVD process: annealing + growth. Fig. 4(e–h) display the SEM images of nanotubes grown on the corresponding annealed substrates in Fig. 4(a–d). It can be seen that nanotubes are less aligned and their densities are terribly low. However, this is in consistent with the nanoparticle densities shown in Fig. 4(a–d). In Fig. 4b, even the highest density obtained from the 0.6 nm Fe sublayer can only approach $10^{11}cm^{-2}$ and it further drops down by half with the 1.8 nm Fe sublayer. As the overall density is much lower than that achieved by the single-step CVD process (Fig. 1(j–k)); it indicates that even a simple pre-annealing in H_2 had already resulted in catalyst loss and/or nanoparticle coarsening on the surface. A CVD process possessing a slow ramping rate may have the same negative effects as annealing. This is the main reason why we chose the single-step cold-wall CVD, which has the ability to heat the substrate to growth temperature in 2–3 min. Single-step CVD also shows advantages on large scale and reproducible growth of aligned CNT forests over multi-step CVD.

It is believed that a higher density of CNT forests is resulted from a higher density of catalytic nanoparticles. In addition to the novel catalyst design, the high concentration of C_2H_2 (8%), which has been proven to be the key growth precursor, [6] could probably have also played a very important role. Yamazaki et al. [31] and Zhang et al. [43] have reported that a proper pretreatment of a catalytic thin film by CH_4 or C_2H_2 plasma could promote the formation of high density catalytic nanoparticles, which are effectively immobilized by a carbon nano-film, leading to the growth of closely packed MWNT forests without causing the catalyst poisoning. High

concentration C_2H_2 is also critical to grow ultra-high-density SWNT forests as reported in our previous study [14]. It is probably the same in our case. Once high density catalytic nanoparticles are formed on substrates with our novel catalyst design during the rapid ramping period, they are immediately immobilized and nucleated to grow nanotubes in the presence of C_2H_2, hindering them from further coarsening or loss through surface and bulk diffusion. However, it is hard to obtain any direct evidence of the density of nanoparticles as the two-step CVD process does.

3.4. *Density evaluation of aligned CNT forests*

For the well aligned CNT forests, we used the liquid-induced compaction for fast density evaluation. Fig. 5 shows some comparative SEM images of the four samples shown in Fig. 1(f–g and j–k) after compaction. Two different microstructures were formed. For the low density samples (Fig. 5(a and b)), a cellular structure is usually formed, which agrees with that of low density MWCNT forests [35–37]. Due to the low density, most of the nanotubes were collapsed and densified on the surface except for those met from opposite directions forming the cell boundaries. For the high density CNT forests, CNT islands would be formed after densification (Fig. 5(c and d)). This is similar to our previous report for ultra-high-density SWCNT forests [14]. From these islands, a filling factor η termed as the area ratio of total islands to the substrate can be obtained, as labeled in Fig. 5(c and d). The higher is the filling factor, the higher is the CNT density. For the best of our samples, a filling factor as high as $\eta = 57\%$ can be reached. Fig. 6(a and b) show the top-view and cross-sectional SEM images of such a sample, while Fig. 6(c and d) are the high resolution SEM images taken before and after the liquid-induced compaction. SEM observations under high magnifications disclose that well aligned and high-density nanotubes were almost compacted into solid blocks (Fig. 6d).

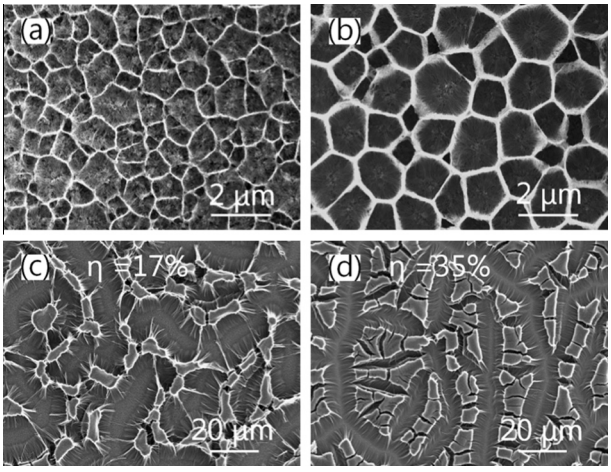

Fig. 5 – Top-view images (a–d) of the CNT forest samples shown in Fig. 1(f–g and j–k) after liquid-induced compaction by soaking the samples thoroughly in ethanol and letting them dry in the air. The nanotube filling factors *g* were also given in (c–d).

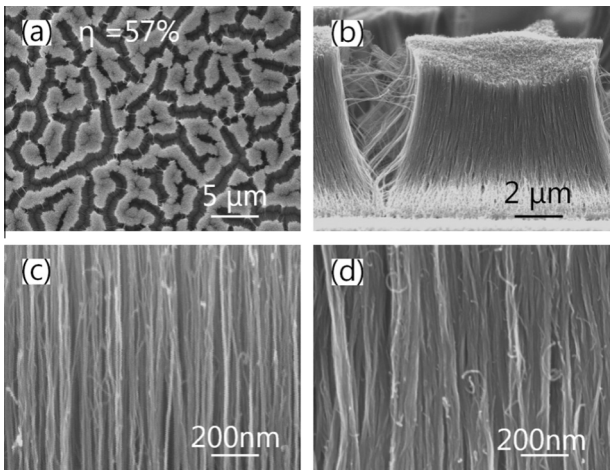

Fig. 6 – SEM images of one CNT forest sample showing the best alignment and highest density of nanotubes. (a) Top-view and (b) cross-sectional SEM images of the sample after liquid-induced compaction. (c and d) High resolution cross-sectional SEM images before and after the compaction.

HRTEM observations reveal that the as-grown high-density CNT forests mainly consist of double-walled and triple-walled nanotubes with a mean diameter of 6.0 nm, as shown in Fig. 7. As we know that the areal density ρ of a nanotube forest is given by [12]:

$$\rho = \frac{1}{S} = \frac{2}{\sqrt{3}(D+\Delta)^2}$$

where, S is the average area occupied by one nanotube; D is the mean diameter of the nanotubes, and Δ is the average wall to wall spacing. The filling factor relates the density of nanotubes before and after the compaction as:

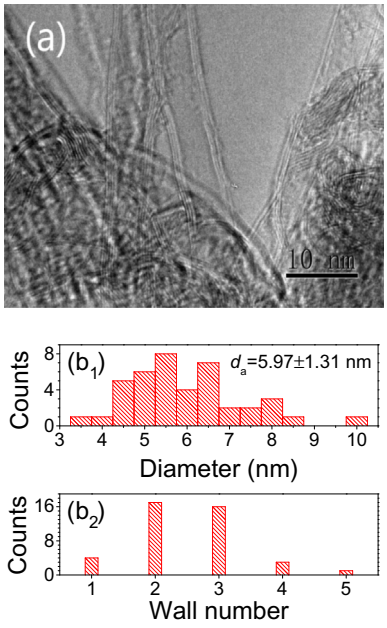

Fig. 7 – HRTEM images of the high-density CNT forests and the diameter/wall number distributions. (A colour version of this figure can be viewed online.)

$$\eta = \frac{S_1}{S_0} = \frac{\rho_0}{\rho_1}$$

where, the subscripts of 0 and 1 represent the states before and after compaction, respectively. The density upper limit for nanotubes with a diameter of 6.0 nm can be calculated from ideally close-packed CNT forests [12], which is 2.87×10^{12} cm^{-2}. Previous study has shown that compacted CNT forests could have a density up to 73% of that of ideally close-packed nanotubes [38]. Here we estimate a density close to 10^{12} cm^{-2} for our best samples prepared. This is similar to Yamazaki et al. work [31], which showed a slightly larger mean CNT diameter of 6–7 nm, and an estimated filling factor of 30–40%. There may still have some room for density improvement by further optimizing the catalyst/metal support/catalyst nanostructure and adopting plasma-assisted catalytic nanoparticle formation and immobilization [31,43].

SEM observation also shows that high-density CNT forests could only grow a few microns in height. We find this is a common feature for CNT forests with high filling factors [14,31,43]. The most probable reason is that a high filling factor means very high packing density of nanotubes, which will strongly block the growth precursors from reaching the catalytic nanoparticles localized at the nanotube/support interface.

4. Summary

In summary, catalyst engineering, by adding an additional catalyst sublayer to the conventional catalyst/support design, is a very efficient way to promote the growth of high-density CNT forests on metal support. In our case, the surface catalyst can be minimized to 0.6–0.8 nm and sustained without remarkable loss or gain during the growth of CNT forests by adding a sublayer of 0.6–0.8 nm Fe catalyst beneath the 10 nm Ti coating. SIMS depth profile analysis and SEM observation indicate that the catalyst diffusion back to the surface from the sublayer overtake that down to the sublayer from the surface. HRTEM observations show that the high-density CNT forests consist of mainly double-walled and triple-walled nanotubes with a mean diameter of 6.0 nm. By using the liquid-induced compaction method, a filling factor up to 57% was achieved, and areal density around 10^{12} cm^{-2} was estimated for our best samples.

Acknowledgement

The authors are grateful to the EC funding of Viacarbon and Technotubes projects.

REFERENCES

[1] Li WZ, Xie SS, Qian LX, Chang BH, Zou BS, Zhou WY, et al. Large-scale synthesis of aligned carbon nanotubes. Science 1996;274(5293):1701–3.
[2] Ren ZF, Huang ZP, Xu JW, Wang JH, Bush P, Siegal MP, et al. Synthesis of large arrays of well-aligned carbon nanotubes on glass. Science 1998;282(5391):1105–7.
[3] Hata K, Futaba DN, Mizuno K, Namai T, Yumura M, Iijima S. Water-assisted highly efficient synthesis of impurity-free single-walled carbon nanotubes. Science 2004;306(5700):1362–4.
[4] Hart AJ, Slocum AH. Rapid growth and flow-mediated nucleation of millimeter-scale aligned carbon nanotube structures from a thin-film catalyst. J Phys Chem B 2006;110(16):8250–7.
[5] Zhong GF, Iwasaki T, Robertson J, Kawarada H. Growth kinetics of 0.5 cm vertically aligned single-walled carbon nanotubes. J Phys Chem B 2007;111(8):1907–10.
[6] Zhong G, Hofmann S, Yan F, Telg H, Warner JH, Eder D, et al. Acetylene: a key growth precursor for single-walled carbon nanotube forests. J Phys Chem C 2009;113(40):17321–5.
[7] Zhang Q, Huang JQ, Zhao MQ, Qian WZ, Wei F. Carbon nanotube mass production: principles and processes. ChemSusChem 2011;4(7):864–89.
[8] Noda S, Hasegawa K, Sugime H, Kakehi K, Zhang ZY, Maruyama S, et al. Millimeter-thick single-walled carbon nanotube forests: hidden role of catalyst support. Jpn J Appl Phys 2007;46(17–19):L399–401.
[9] Mattevi C, Wirth CT, Hofmann S, Blume R, Cantoro M, Ducati C, et al. In-situ x-ray photoelectron spectroscopy study of catalyst–support interactions and growth of carbon nanotube forests. J Phys Chem C 2008;112(32):12207–13.
[10] Sakurai S, Nishino H, Futaba DN, Yasuda S, Yamada T, Maigne A, et al. Role of subsurface diffusion and ostwald ripening in catalyst formation for single-walled carbon nanotube forest growth. J Am Chem Soc 2012;134(4):2148–53.
[11] Robertson J, Zhong GF, Esconjauregui CS, Bayer BC, Zhang C, Fouquet M, et al. Applications of carbon nanotubes grown by chemical vapor deposition. Japn J Appl Phys 2012;51(1):01AH01.
[12] Zhong GF, Iwasaki T, Kawarada H. Semi-quantitative study on the fabrication of densely packed and vertically aligned single-walled carbon nanotubes. Carbon 2006;44(10):2009–14.
[13] Esconjauregui S, Fouquet M, Bayer BC, Ducati C, Smajda R, Hofmann S, et al. Growth of ultrahigh density vertically aligned carbon nanotube forests for interconnects. Acs Nano 2010;4(12):7431–6.
[14] Zhong GF, Warner JH, Fouquet M, Robertson AW, Chen BA, Robertson J. Growth of ultrahigh density single-walled carbon nanotube forests by improved catalyst design. ACS Nano 2012;6(4):2893–903.
[15] Sakurai S, Inaguma M, Futaba DN, Yumura M, Hata K. Diameter and density control of single-walled carbon nanotube forests by modulating ostwald ripening through decoupling the catalyst formation and growth processes. Small 2013. http://dx.doi.org/10.1002/smll.201300223.
[16] Robertson J, Zhong G, Telg H, Thomsen C, Warner JM, Briggs GAD, et al. Carbon nanotubes for interconnects in vlsi integrated circuits. Phys Status Solidi B-Basic Solid State Phys 2008;245(10):2303–7.
[17] Robertson J, Zhong G, Hofmann S, Bayer BC, Esconjauregui CS, Telg H, et al. Use of carbon nanotubes for vlsi interconnects. Diamond Relat Mater 2009;18(5–8):957–62.
[18] Horibe M, Nihei M, Kondo D, Kawabata A, Awano Y. Carbon nanotube growth technologies using tantalum barrier layer for future ulsis with cu/low-k interconnect processes. Japn J Appl Phys Part 1 Regular Pap Brief Commun Rev Pap 2005;44(7A):5309–12.
[19] Bayer BC, Zhang C, Blume R, Yan F, Fouquet M, Wirth CT, et al. In-situ study of growth of carbon nanotube forests on conductive cosi2 support. J Appl Phys 2011;109(11):114314.
[20] Zhang C, Yan F, Allen CS, Bayer BC, Hofmann S, Hickey BJ, et al. Growth of vertically-aligned carbon nanotube forests on conductive cobalt disilicide support. J Appl Phys 2010;108(2):024311.

[21] Nessim GD, Acquaviva D, Seita M, O'Brien KP, Thompson CV. The critical role of the underlayer material and thickness in growing vertically aligned carbon nanotubes and nanofibers on metallic substrates by chemical vapor deposition. Adv Funct Mater 2010;20(8):1306–12.
[22] Bayer BC, Hofmann S, Castellarin-Cudia C, Blume R, Baehtz C, Esconjauregui S, et al. Support–catalyst–gas interactions during carbon nanotube growth on metallic ta films. J Phys Chem C 2011;115(11):4359–69.
[23] Kim HS, Kim B, Lee B, Chung H, Lee CJ, Yoon HG, et al. Synthesis of aligned few-walled carbon nanotubes on conductive substrates. J Phys Chem C 2009;113(42):17983–8.
[24] Parthangal PM, Cavicchi RE, Zachariah MR. A generic process of growing aligned carbon nanotube arrays on metals and metal alloys. Nanotechnology 2007;18(18):185605.
[25] Kim SM, Gangloff L. Growth of carbon nanotubes (cnts) on metallic underlayers by diffusion plasma-enhanced chemical vapour deposition (dpecvd). Physica E Low Dimens Syst Nanostruct 2009;41(10):1763–6.
[26] Dorfler S, Meier A, Thieme S, Nemeth P, Althues H, Kaskel S. Wet-chemical catalyst deposition for scalable synthesis of vertical aligned carbon nanotubes on metal substrates. Chem Phys Lett 2011;511(4–6):288–93.
[27] Bult JB, Sawyer WG, Ajayan PM, Schadler LS. Passivation oxide controlled selective carbon nanotube growth on metal substrates. Nanotechnology 2009;20(8):085302.
[28] Lepro X, Lima MD, Baughman RH. Spinnable carbon nanotube forests grown on thin, flexible metallic substrates. Carbon 2010;48(12):3621–7.
[29] Hiraoka T, Yamada T, Hata K, Futaba DN, Kurachi H, Uemura S, et al. Synthesis of single- and double-walled carbon nanotube forests on conducting metal foils. J Am Chem Soc 2006;128(41):13338–9.
[30] Zhang C, Yan F, Bayer BC, Blume R, van der Veen MH, Xie RS, et al. Complementary metal-oxide-semiconductor-compatible and self-aligned catalyst formation for carbon nanotube synthesis and interconnect fabrication. J Appl Phys 2012;111(6):064310.
[31] Yamazaki Y, Katagiri M, Sakuma N, Suzuki M, Sato S, Nihei M, et al. Synthesis of a closely packed carbon nanotube forest by a multi-step growth method using plasma-based chemical vapor deposition. Appl Phys Expr 2010;3(5):055002.
[32] Dijon J, Okuno H, Fayolle M, Vo T, Pontcharra J, Acquaviva D, et al. Ultra-high density carbon nanotubes on al–cu for advanced vias. IEEE International In: Electron Devices Meeting (IEDM), 2010. p. 33.4.1–4.4.
[33] Esconjauregui S, Xie RS, Guo YZ, Pfaendler SML, Fouquet M, Gillen R, et al. Electrical conduction of carbon nanotube forests through sub-nanometric films of alumina. Appl Phys Lett 2013;102(11):113109.
[34] Rao R, Chen G, Arava LMR, Kalaga K, Ishigami M, Heinz TF, et al. Graphene as an atomically thin interface for growth of vertically aligned carbon nanotubes. Sci Rep 2013;3:01891.
[35] Liu H, Li SH, Zhai J, Li HJ, Zheng QS, Jiang L, et al. Self-assembly of large-scale micropatterns on aligned carbon nanotube films. Angew Chem Int Ed 2004;43(9):1146–9.
[36] Chakrapani N, Wei BQ, Carrillo A, Ajayan PM, Kane RS. Capillarity-driven assembly of two-dimensional cellular carbon nanotube foams. Proc Natl Acad Sci USA 2004;101(12):4009–12.
[37] Correa-Duarte MA, Wagner N, Rojas-Chapana J, Morsczeck C, Thie M, Giersig M. Fabrication and biocompatibility of carbon nanotube-based 3d networks as scaffolds for cell seeding and growth. Nano Lett 2004;4(11):2233–6.
[38] Futaba DN, Hata K, Yamada T, Hiraoka T, Hayamizu Y, Kakudate Y, et al. Shape-engineerable and highly densely packed single-walled carbon nanotubes and their application as super-capacitor electrodes. Nat Mater 2006;5(12):987–94.
[39] Fan SS, Chapline MG, Franklin NR, Tombler TW, Cassell AM, Dai HJ. Self-oriented regular arrays of carbon nanotubes and their field emission properties. Science 1999;283(5401):512–4.
[40] Xu M, Futaba DN, Yumura M, Hata K. Alignment control of carbon nanotube forest from random to nearly perfectly aligned by utilizing the crowding effect. ACS Nano 2012;6(7):5837–44.
[41] Esconjauregui S, Bayer BC, Fouquet M, Wirth CT, Yan F, Xie R, et al. Use of plasma treatment to grow carbon nanotube forests on tin substrate. J Appl Phys 2011;109(11):114312.
[42] Sugime H, Esconjauregui S, Yang J, D'Arsie L, Oliver RA, Bhardwaj S, et al. Low temperature growth of ultra-high mass density carbon nanotube forests on conductive supports. Appl Phys Lett 2013;103(7):073116.
[43] Zhang C, Xie R, Chen B, Yang J, Zhong G, Robertson J. High density carbon nanotube growth using a plasma pretreated catalyst. Carbon 2013;53:339–45.